Article:

Bállico, MB, Scherer, CMS, Mountney, NP orcid.org/0000-0002-8356-9889 et al. (4 more authors) (2017) Sedimentary cycles in a Mesoproterozoic aeolian erg-margin succession: Mangabeira Formation, Espinhaço Supergroup, Brazil. Sedimentary Geology, 349. pp. 1-14. ISSN 0037-0738

https://doi.org/10.1016/j.sedgeo.2016.12.008

Accepted Manuscript

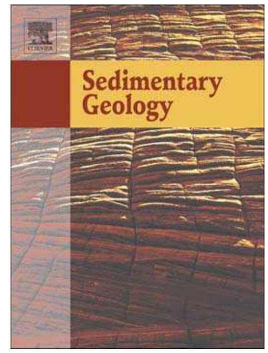

Sedimentary cycles in a Mesoproterozoic aeolian erg-margin succession: Mangabeira Formation, Espinhaço Supergroup, Brazil

M.B. Bállico, C.M.S. Scherer, N.P. Mountney, E.G. Souza, A.D. Reis, G.P. Raja Gabaglia, A.J.C. Magalhães

PII: S0037-0738(16)30314-1
DOI: doi:10.1016/j.sedgeo.2016.12.008
Reference: SEDGEO 5149

To appear in: *Sedimentary Geology*

Received date: 30 September 2016
Revised date: 24 December 2016
Accepted date: 26 December 2016

Please cite this article as: Bállico, M.B., Scherer, C.M.S., Mountney, N.P., Souza, E.G., Reis, A.D., Raja Gabaglia, G.P., Magalhães, A.J.C., Sedimentary cycles in a Mesoproterozoic aeolian erg-margin succession: Mangabeira Formation, Espinhaço Supergroup, Brazil, *Sedimentary Geology* (2016), doi:10.1016/j.sedgeo.2016.12.008

Sedimentary cycles in a Mesoproterozoic aeolian erg-margin succession: Mangabeira Formation, Espinhaço Supergroup, Brazil

M.B. Bállico[a*], C.M.S. Scherer[a], N.P. Mountney[b], E.G. Souza[a], A.D. Reis[a], G.P. Raja Gabaglia[c], A.J.C. Magalhães[c]

[a] Universidade Federal do Rio Grande do Sul – Instituto de Geociências, 9500 Bento Gonçalves Avenue, 91501-970, Porto Alegre, Brazil

[b] Fluvial & Eolian Research Group, School of Earth and Environment, University of Leeds, United Kingdom, LS2 9JT, UK

[c] Petróleo Brasileiro SA, PETROBRAS, Rio de Janeiro, RJ, Brazil

* Corresponding author: Universidade Federal do Rio Grande do Sul – Instituto de Geociências, 9500 Bento Gonçalves Avenue, 91501-970, Porto Alegre, Brazil

+55 51 3308 6372 Phone

+55 51 3308 7047 Fax

manoela.bettarel@gmail.com

Abstract

Aeolian systems were abundant and widespread in the early Proterozoic, post-2.2 Ga. However, the majority of aeolian successions of such great age are intensely deformed and are preserved only in a fragmentary state meaning that, hitherto, few attempts have been made to apply a sequence stratigraphic approach to determine mechanisms of aeolian construction, accumulation and preservation in such systems. The Mangabeira Formation is a well preserved Mesoproterozoic erg successions covering part of the São Francisco Craton, northeastern Brazil. The lower unit of the Mangabeira Formation (~500 m thick) comprises aeolian deposits of dune, interdune, and sand-sheet origin, as well as some of waterlain origin. These deposits are organized into vertically stacked depositional cycles, each 6 to 20 m thick, and characterized by aeolian sandsheet and waterlain deposits succeeded by aeolian dune and interdune deposits indicative of a drying-upward trend. Aeolian cross-strata exhibit a mean dip direction to the north. Each of these cycles likely arose in response to climatic oscillation from relatively humid to arid conditions, possibly related to orbital forcing. The lower unit of the Mangabeira Formation comprises up to 14 erg sequences. The accumulation and preservation of each was determined by the relative rate of water-table rise and the availability of sand for aeolian transport, both of which changed through time, resulting in the preservation of a succession of repeated drying-upward cycles.

Keywords: Mesoproterozoic age; aeolian succession; erg margin; drying-upward cycles; climatic oscillations

1. Introduction

The recognition of aeolian deposits and the interpretation of palaeoenvironments of aeolian origin in Precambrian successions may be attempted through the implementation of techniques of facies analysis, although the deformed and fragmentary state of preservation of the great majority of outcropping successions of this age make such analysis challenging. Study techniques involve the identification of diagnostic sedimentary structures and textures indicative of aeolian processes, including various types of cross-bedded sets composed internally of various arrangements of wind-ripple, grainflow and grainfall strata, and intervening, horizontally laminated sets of wind-ripple, adhesion and granule-ripple strata (Kocurek, 1996; Mountney, 2006). Although Precambrian aeolian successions are well documented (Eriksson and Simpson, 1998; Rodríguez-López et al., 2014), relatively few studies have undertaken a detailed analysis of the facies architecture of these aeolian successions with the aim of gaining an improved comprehension of the stratigraphic evolution and palaeoenvironment (Ross, 1983; Jackson et al., 1990; Chakraborty, 1991; Simpson and Eriksson, 1993; Basu et al., 2014; Heness et al., 2014). Studies of Proterozoic successions are notably important for determining aeolian-system dynamics that prevailed prior to the evolution of land plants; results of such studies find direct application to gaining an improved understanding of sedimentary processes that prevailed on other planets, for example aeolian processes on Mars, where different ancient (Grotzinger et al., 2005) and recent deposits (Sullivan et al., 2005; Hayes et al., 2011) of aeolian dunes have been identified.

The aim of this study is to undertake a lithofacies and architectural-element analysis of aeolian and related deposits of the Mangabeira Formation to reconstruct the detailed palaeoenvironment of this ancient desert system and thereby determine the controls that gave rise to its accumulation and preservation. Specific research objectives of this study are as follows: (i) to employ lithofacies and architectural-element analysis to reconstruct and interpret the various aeolian sub-environments represented by the preserved aeolian sequences; (ii) to propose a depositional model for the evolution of the Mangabeira Formation; and (iii) to discuss the main variables that controlled the construction, accumulation and preservation this Proterozoic aeolian succession.

2. Background

To understand the palaeoenvironmental significance of preserved aeolian sedimentary architecture, and to attempt a detailed palaeoenvironmental reconstruction, determination of three phases of aeolian system evolution is required: aeolian system construction, accumulation and preservation (Kocurek, 1999; Kocurek and Lancaster, 1999). In many studies of Phanerozoic aeolian successions, preserved aeolian accumulations are commonly divided into sequences, each of which represents a phase of aeolian construction and accumulation. These sequences commonly occur vertically stacked to form a succession, whereby each sequence is delimited by a laterally extensive supersurface that marks a hiatus in the accumulation process, and which may be associated with evidence indicative of aeolian deflation (i.e. net erosion) (Loope, 1985; Kocurek and Hunter, 1986; Langford and Chan, 1988; Clemmensen and Hegner, 1991; Mountney et al., 1999; Scherer and Lavina, 2005; Mountney, 2006). Thus, supersurfaces are types of sequence boundaries (Kocurek, 1988). The recognition of supersurfaces forms the basis for defining a sequence stratigraphic framework for aeolian successions. However, the recognition of supersurfaces in Precambrian aeolian successions, as well as the construction of models related to the spatial and temporal evolution of the aeolian units, has not been widely attempted previously (see Deynoux et al., 1989). Aeolian successions of Precambrian age are typically highly fragmentary such that they lack the lateral continuity of exposure required to demonstrate the relationships between sequences and their bounding supersurfaces. Furthermore, subtle lithofacies relationships are typically not well preserved in these ancient – and commonly deformed and metamorphosed – successions (Eriksson and Simpson, 1998; Bose et al., 2012).

Individual supersurfaces and the sequences that they bound commonly extend over large geographic areas, and correspond to individual and distinct aeolian ergs (dune fields) that were constructed and accumulated. Individual sequences represent the preserved deposits of distinct ergs, each of which may be separated from neighbouring erg sequences in both space and time (Kocurek, 1988). The supersurfaces that bound these sequences represent hiatuses in aeolian accumulation (Loope, 1985; Clemmensen et al., 1989; Deynoux et al., 1989; Kocurek et al., 1991a; Lancaster, 1992). Supersurfaces serve as the basis for the definition of the limits of aeolian genetic units. Lithofacies arrangements within these aeolian genetic units yield information about the process of sedimentation. Assemblages (associations) of lithofacies are themselves contained within elements that represent the individual components (architectural elements) of aeolian systems, such as dunes of different morphological types, interdunes and sand flats. Architectural elements provide information about the morphology of the original sedimentary sub-environments, and the main controls on their accumulation and preservation (Havholm and Kocurek, 1994; Veiga et al., 2002; Scherer and Lavina, 2005; Mountney, 2006).

3. Geological Setting

The São Francisco Craton is located in northeast Brazil (Fig. 1a) and comprises Archean/Palaeoproterozoic basement rocks composed of metamorphic and supracrustal rocks, which are overlain by a Palaeoproterozoic to Phanerozoic sedimentary cover succession (e.g., Almeida, 1977; Barbosa et al., 2004; Cruz and Alkmim, 2006; Alkmim and Martins-Neto, 2012). One the main physiographic feature of the São Francisco Craton is the Chapada Diamantina Range (Fig. 1b). Here, the Espinhaço Supergroup and the São Francisco Supergroup are the main sedimentary units: the former is of Palaeoproterozoic to Neoproterozoic age and principally comprises siliciclastic rocks; the latter is characterized mainly by carbonate successions of Neoproterozoic age (Fig. 1b).

The Espinhaço Supergroup spans an age range from c. 1.75 to 0.9 Ga based on radiometric age constraints (Schobbenhaus et al., 1994; Babinski et al., 1999) (Fig. 2). This unit is composed principally of clastic sedimentary rocks of continental and coastal origin (Alkmim and Martins-Neto, 2012; Danderfer et al., 2009; Pedreira and de Waele, 2008), and associated volcanic deposits (Schobbenhaus et al., 1994; Babinski et al., 1999). The full Espinhaço succession comprises three megasequences termed the Lower, Middle and Upper sequences (Chemale et al., 2012; Santos et al., 2013; Guadagnin et al., 2015b) (Fig. 2) . These megasequences accumulated in numerous basins developed in response to at least two phases of rifting.

The Lower Megasequence (1.8 to 1.68 Ga) is characterized by alkaline, acid volcanism followed by siliciclastic deposition (Fig. 2); these deposits form the majority of the fill of a series of rift basins (Guimarães et al., 2008; Alkmim and Martins-Neto, 2012). The overlying and stratigraphically younger Middle Espinhaço Megasequence comprises continental and coastal deposits (Fig. 2) deposited during the Calymmian (1.6 to 1.38 Ga) (Pedreira, 1994; Guimarães et al., 2008; Pedreira and de Waele, 2008; Alkmim and Martins-Neto, 2012; Guadagnin et al., 2015a, 2015b). This megasequence is represented by the Mangabeira, Açuruá and Tombador formations.

Of these, the Mangabeira Formation is the focus of this study. This unit was defined by Schobbenhaus and Kaul (1971) and interpreted by Pedreira (1994); it records the accumulation of a palaeo-desert environment, with aeolian dunes and wadi deposits. The Mangabeira Formation has a radiometric age date ca. 1.5 Ga, based on dates derived from mafic sills and dyke swarms that cut the base of the formation (Babynski et al., 1999; Silveira et al., 2013). The Lower Unit of the Mangabeira Formation crops out over ~50.000 km^2 across the São Francisco Craton. The outcrops of this unit examined for this study are located in the southern area (~1200 km^2) of the Chapada Diamantina Domain (Fig. 1c), where outcrops tat reveal subtle sedimentary structures are best preserved. Other areas of the São Francisco Craton have been subject to intensive deformation and metamorphism, rendering the succession elsewhere unsuitable for sedimentary lithofacies and sequence stratigraphic analysis. The basal contact between the underlying Lagoa de Dentro Formation and the Mangabeira Formation is not exposed in the studied area. The upper contact with the overlying Açuruá Formation is sharp.

4. Methods

In the Mangabeira Formation, 11 detailed graphic sedimentological sections with a total combined thickness of ~500 m were measured at 1:100 scale. These logs record grain size, physical sedimentary structures and palaeocurrent data (281 readings). Palaeocurrents were determined from the dip azimuths of foresets present in cross-bedded sandstone sets (Fig. 3). The azimuth and dip angle of the dune foresets were later corrected to remove the effects of structural tilt. A series of two-dimensional panels detail the sedimentary features of a 480 m-long outcrop section. Five ground-penetrating radar (GPR) survey lines, which are collectively 3.3 km long, image the geometry of preserved sets. The GPR lines were collected in front of the outcrops along a roadside section. These data have assisted in the establishment of geometric relationships between facies associations. The GPR data were collected using a Subsurface Interface Radar (SIR) 3000 system developed by Geophysical Survey System, Inc. (GSSI), using 200 and 400 MHz antennae. Position and local topography was determined using a Global Positioning System (GPS) survey; spatial resolution was 0.1 m. The processing of these data was undertaken using *Reflexw 6.1* software.

5. Results

Four distinct facies associations are identified in the deposits of the Lower Unit of the Mangabeira Formation and these are each ascribed to a particular sub-environment (Table 1): aeolian dune (A1), aeolian interdune (A2), aeolian sand sheet (A3), and fluvial (A4).

5.1. Aeolian Dune Association (A1)

5.1.1. Description

This facies association comprises fine- to medium-grained sandstone composed of grains that are well-rounded to sub-rounded, well-sorted or in some cases bimodally sorted. The sandstone deposits are arranged into cross-stratified sets, each 0.2 to 1.5 m thick. The majority of sets are characterized internally by foresets inclined at 20 to 25º relative to set bases. These cross-beds form wedges of sand flow (i.e., grainflow) strata, each 10 to 80 mm thick (Fig. 4a), that pinch out down-dip where they are interbedded with deposits of 5 to 10 mm-thick wind-ripple laminae (Fig. 4b). The sandstone bodies occur as co-sets of strata that are themselves 0.2 to 3 m thick, and which are arranged into tabular sand bodies that have lateral extents of up to 40 m, and that are defined by sharp boundaries. The individual wedge-shaped sets that comprise these co-sets occur at two distinct scales: 0.2 to 0.5 m thick and up to 1.5 m thick. In orientations transverse to the dip direction of inclined foresets within sets, packages of cross-strata are characterized by trough-shaped bodies, each up to 10 m wide and each delineated by a basal bounding surface. In orientations parallel to the dip direction of inclined foresets, cross-strata are tangential to planar basal bounding surfaces, which are themselves near-horizontal or are inclined gently (<5°) in the direction opposite to the dip of the foresets. Internally, the cross-bedded sets can be subdivided into sub-sets, which are themselves bounded by inclined surfaces that dip up to 15º. These surfaces truncate the cross-strata below but overlying cross-strata above are concordant (Fig. 4c). These inclined surfaces are bounded by gentle/near horizontal, downwind dipping surfaces. Foreset dip azimuths are variable in the range to 045º to 335º. Most foresets dip <20º, though inclinations vary from 18º to 40º in some places. The lower and upper boundaries that define larger packages of strata comprising this facies association are abrupt and planar.

5.1.2. Interpretation

The trough cross-stratification combined with well-sorted and well-rounded texture of the sand grains, and the presence of grainflow and wind-ripple laminae indicates deposition from migrating aeolian dunes (Hunter, 1977). The common trough-tangential pattern of cross-stratification combined with high dispersion values of the foreset dip azimuths indicates deposition of 3D-crescentic bed forms (Fig. 3). The presence of grainflow strata indicated by foresets present in the upper parts of preserved sets indicates that bed forms possessed well-developed slipfaces (Hunter, 1977). The down-dip pinch of the grainflow strata and their interfingering with wind-ripple lamination in the lower parts of sets demonstrate that lee-slope grainflow avalanches reached the toesets of the bed forms. Wind ripples migrated over the dune plinths (Scherer, 2000; Mountney, 2006). The near-horizontal to low-angle surfaces inclined in the direction opposite to the dip of the foresets observed in sections oriented parallel to palaeoflow are interpreted as interdune migration surfaces formed through the climbing of aeolian dunes (Kocurek, 1996). The trough-shaped geometry of the interdune surfaces observed in orientations transverse to palaeoflow indicates that the main bedform crestlines were high sinuous. The stacking of numerous sets bounded by trough-shaped interdune surfaces indicates the migration of successive, out-of-phase sinuous aeolian dunes (Rubin, 1987). The inclined bounding surfaces that occur internally within cross-bedded sets and which dip in a similar direction to the cross-strata are most readily interpreted as reactivation surfaces (Kocurek, 1996). These surfaces indicate partial lee-side erosion during minor changes in wind direction and/or strength (Brookfield, 1977; Rubin and Hunter, 1982; Hunter and Rubin, 1983; Scherer and Lavina, 2005; Mountney, 2006). These reactivation surfaces are themselves truncated by interdune surfaces (Kocurek, 1981a, 1991).

5.2. Aeolian Interdune Association (A2)

5.2.1. Description

This facies association comprises sandstone composed of grains that are well-sorted and well-rounded to sub-rounded. The sandstone occurs as irregular beds that are each 0.1 to 0.2 m thick and 10 to 20 m in lateral extent (Fig. 5a, 5b). Two types of structures are identified in this facies association. The first is represented by very fine- to fine-grained sandstone identified by 5 to 10 mm-thick, inversely graded, horizontal lamination that forms translatent strata (*sensu* Hunter, 1977) (Fig. 5c, 5d). The second is represented by very fine- to fine-grained sandstone packages that are each 0.5 to 10 cm thick and which alternate with 10 to 30 mm-thick irregular mudstone laminae to form wavy and corrugated (crinkly) lamination (Fig. 5d, 5e). At a larger scale, these deposits occur intercalated with aeolian dune cross-strata of association A1. The basal bounding surfaces that delineate accumulations of association A2 are sharp and commonly slightly erosive; the upper bounding surfaces are sharp but non-erosional (Fig. 5a).

5.2.2. Interpretation

The occurrence of laterally discontinuous and irregular beds of translatent strata, and wavy and corrugated lamination, and their intercalation with aeolian dune cross-strata accumulations of association A1 indicates a facies association typical of an aeolian interdune setting (Mountney, 2006). The two sedimentary structures types indicate that the interdune deposits accumulated in response to two types of substrate condition. The inversely graded, horizontal lamination (translatent strata) arose in response to the subcritical climb of wind-ripple strata (Hunter, 1977), and is indicative of accumulation on a dry substrate where the water table and its capillary fringe lay beneath the accumulation surface. The wavy and corrugated (crinkly) lamination is most obviously interpreted as the preserved product of adhesion structures accumulated on a damp substrate, and indicates a setting where the water table was located close to the accumulation surface (Kocurek and Fielder, 1982; Mountney and Thompson, 2002; Paim and Scherer, 2007). A possible alternative interpretation for the corrugated (crinkly) lamination is a microbial origin. Souza (2012) described several types of wavy and wrinkle lamination features in the aeolian interdune deposits of the Mangabeira Formation and interpreted them as microbially induced sedimentary structures (MISS). Such MISS structures are syndepositional features formed by the interaction of biofilms or microbial mats with the physical sediment in aquatic environments (Noffke, 2010). The occurrence of MISS in Precambrian aeolian deposits has also been observed previously by other workers, including, for example, by Sarkar et al. (2008) in the Neo-proterozoic Sonia Sandstone (India) and by Eriksson et al. (2000) in the Palaeo-proterozoic Waterberg Group (South Africa). The latter authors described muddy roll-up structures in damp interdune settings where ephemeral ponds are thought to have enabled the establishment of microbial communities. The thin interdune deposits of association A2 described here are indicative of dry and damp interdune hollows or corridors present between the aeolian dunes represented by deposits of association A1. The small preserved thickness and limited lateral extent of the interdune deposits likely indicates that they accumulated in isolated interdune hollows surrounded by dunes (cf., Mountney and Jagger, 2004).

5.3. Aeolian Sandsheet Association (A3)

5.3.1. Description

This facies association comprises very-fine- to medium-grained sandstone, grains of which are moderately sorted. These sandstones are arranged into sets characterized by low-angle-inclined stratification (<5º). These sets are 0.6 to 6 m thick and have a tabular geometry with a lateral extent up to 50 m. Internally, these sets are characterized by several structures which occur interlayered in the studied sections as packages of strata that vary from 0.6 to 1 m thick. The main lithofacies are: (i) 5 to 10 mm-thick, inverse graded, horizontally to low-angle translatent lamination arranged into sets that are themselves 0.1 to 0.2 m thick (Fig. 6a); (ii) tangential cross-stratified sandstones that form lenticular and laterally discontinuous sets up to 0.2 m thick (Fig. 6b), and which are formed entirely by inverse graded lamination; and (iii) 5 to 20 mm-thick packages of interlayered sandstone and mudstone, with crinkly lamination, in sets that are 50 to 100 mm thick and which are laterally traceable for up to 10 m (Fig. 6c). These deposits both overlie and are themselves overlain by the aeolian dune deposits of association A1; bounding surfaces are sharp and horizontal. These deposits commonly occur intercalated with waterlain deposits of association A4 (see below).

5.3.2. Interpretation

The tabular sandstones with low-angle-inclined stratification are interpreted as aeolian sandsheet accumulations. The thin, horizontal to low-angle-inclined translatent strata with inverse grading laminae represent ripple deposits formed by the migration and climbing of wind ripples over a dry depositional surface (Hunter, 1977). The tangential cross-beds are interpreted as small aeolian dunes; the laterally discontinuous extent of the cross-bedded sets, and their style of interlayering with the horizontal to low-angle-inclined wind-ripple strata indicate that these small bed forms migrated and accumulated episodically and fortuitously as local accommodation became available. The deposits of interlayered sandstone and mudstone with the crinkly lamination are interpreted as adhesion-ripple strata. Accumulation of sets of adhesion lamination requires a water-saturated substrate, whereby loose sand grains blown by the wind adhere to a damp or wet surface as they make contact with it, and progressively accumulate (Kocurek and Fielder, 1982; Kocurek and Nielson, 1986; Chakraborty and Chaudhuri, 1993; Scherer and Lavina, 2005). The common and repeated stacking of packages of adhesion strata, translatent wind-ripple strata and waterlain deposits is typical of a sand sheet setting in which the local water table repeatedly fluctuated in level (possibly seasonally), and for which there were temporal changes in the availability of dry sand for aeolian transport (Chakraborty and Chaudhuri, 1993; Scherer and Lavina, 2005).

5.4. Fluvial Association (A4)

5.4.1. Description

This facies association comprises fine- to medium-grained sandstone, grains of which are moderately sorted and characterized by ripple cross-stratification. These sandstones occur as 0.1 m-thick sets (Fig. 6d, 6e), groups of which occur collectively as stacked co-sets that are themselves 1 to 2 m thick and and over 20 m long (outcrop maximum extent). Rare, small-scale (< 0.2 m thick) soft-sediment deformation structures in the form of simple load-cast structures are present on some bedding surfaces. These structures are irregular, in the form of rounded lobes, laterally restrict (Fig. 6f). Thin lenses and drapes of massive mudstone (up to 10 mm thick) are also rarely observed. Accumulations of this association commonly occur in close proximity to the aeolian sandsheet deposits of association A3.

5.4.2. Interpretation

The fine- to medium-grained sandstone with ripple-cross stratification is interpreted as the product of the migration and accumulation of 2D or 3D ripples of subaqueous origin formed in the lower flow regime (Miall, 1977). The minor occurrence of mudstone drapes indicates settling of suspended sediments in a low-energy environment, probably in the aftermath of ephemeral floods (Miall, 2006). The simple load-cast structures were likely generated in response to fluidization in unconsolidated sediments, whereby water-saturated layers lose strength (Owen, 2003).

6. Stratigraphic Architecture: Drying-Upward Cycles

The Lower Unit of the Mangabeira Formation comprises at least 14 stacked, aeolian-dominated sedimentary cycles through the ~500 m-thick succession (Fig. 7). Each accumulated cycle consists of aeolian sandsheet and waterlain deposits that are replaced upward by aeolian dune and interdune deposits. Each cycle is bounded at its base and top by laterally extensive, near-horizontal surfaces. The vertical arrangement of facies defines a drying-upward trend and this trend is repeated within each cycle. The drying-upward cycles recognized in outcrop and in the GPR profile are each 6 to 20 m thick (Fig. 8).

The near-horizontal surfaces that mark the base and top of each cycle are planar and laterally extensive; they can be traced across outcrops and are also evident in the GPR data (Fig. 8). However, in contrast to other examples of similar surfaces documented in the literature (e.g. Loope, 1985; Kocurek and Hunter, 1986; Fryberger et al., 1988; Mountney, 2006; Rodríguez-López et al., 2008), these surfaces are not associated with salt pseudomorphs or other salt-related features, nor calcrete horizons or carbonate cements.

The lowermost deposits of each cycle comprise aeolian sandsheet (A3) and waterlain (A4) deposits in packages of accumulated strata that are 1 to 6 m thick. Internally, the aeolian sandsheet and waterlain deposits comprise arrangements of lithofacies that are themselves arranged into small-scale cycles that comprise adhesion ripples and waterlain deposits overlain upward by wind-ripple and minor, small-scale sets of aeolian dune strata. These deposits of associations A3 and A4 are themselves overlain by aeolian dunes (A1) and interdunes (A2) in the upper part of each depositional cycle.

The uppermost deposits are defined by a set of small-scale sets aeolian cross-strata (5 to 10 m thick) which progressively increase in thickness up-succession to a set of medium- to large-scale sets aeolian cross-strata (5 to 8 m thick). The configuration of aeolian dune and interdune strata is distinct within each cycle (sequence). Most commonly, the succession is characterized by vertically stacked aeolian dune deposits (A1) alone. In such cases, each aeolian dune set is separated from an overlying dune set by a sharp bounding surface, with no evidence of accumulation of interdune deposits. Less commonly, and only in some aeolian sequences, sets of aeolian dunes deposits (A1) occur interbedded with dry or damp interdune deposits of association A2. Such interdune deposits are typically restricted in their lateral extent (10 to 20 m wide).

7. Depositional Model

Throughout the studied ~500 m-thick vertical succession, multiple dry-upward cycles have been observed. The predictable arrangement of facies within each cycle and the repetition of this trend in each of the vertically stacked cycles demonstrate that a repeating set of external controls influenced sediment accumulation in the Lower Unit of the Mangabeira Formation. The drying-upward climatic trends indicated by the deposits of each cycle, and the capping of these cycles by laterally extensive bounding surfaces is the preserved record of distinct phases of accumulation and destruction of an aeolian dune-field (erg) system. Multiple ergs were constructed, accumulated and then partially deflated over time (Fig. 7), as explained below.

Erg dynamics are driven by different factors: (i) the generation and storage of and supply of sediment suitable for aeolian transport; (ii) the availability of dry sand for aeolian transport; (iii) the transport capacity of the wind; and (iv) water table behaviour. The interaction of these controls determines how aeolian systems are constructed, accumulated and eventually preserved over time and space (Kocurek and Havholm, 1993; Kocurek, 1999).

The lowermost deposits in each depositional cycle represent the development of wet aeolian systems in which aeolian sandsheets accumulated in association with waterlain deposits. The dominance of adhesion structures and their close association with wind-ripple strata indicates that a near-surface water table and its capillary fringe controlled the accumulation of these deposits but that its level fluctuated to allow drying of the accumulation surface at times (Cain and Mountney, 2011). Specifically, the small-scale cycles observed within these deposits, in which adhesion-ripple strata and waterlain structures giving way upwards to wind-ripple strata and rare small-scale sets of aeolian-dune strata, indicate that the position of the water table relative to the accumulation surface changed over time (cf., Mountney and Thompson, 2002). During episodes when the water table was relatively low, the availability of dry sand above depositional surface increased, favouring the accumulation of wind-ripple strata. The waterlain deposits of association A4 are typical of accumulation in the aftermath of episodes of intense precipitation, which resulted in fluvial incursion into the erg margin, thereby driving an associated rise in the water-table level (Langford and Chan, 1989; Al-Masrahy and Mountney, 2015). As a consequence, this restricted the availability of dry sand for aeolian transport. This stacking pattern is similar to the cyclically arranged packages of aeolian sandsheet strata described by Chakraborty (1991) in the late Proterozoic Venkatpur Sandstone, India, in which he ascribed deposits to drying-upward cycles recorded in a zone of transition between an erg-margin setting and an aeolian dune-field setting.

Given the Precambrian age of the Mangabeira Formation, the absence of terrestrial vegetation – which in post-vegetation desert system operates as an important runoff inhibitor and sediment-binding mechanism through the development deep root systems – would have resulted in large areas being particularly susceptible to sediment entrainment and reworking by fluvial flash-flood discharge regimes. “Dry" aeolian deposits that lay above the water table would have been particularly susceptible to fluvial reworking (cf., Cain and Mountney, 2011), and would have low preservation potential (Eriksson and Simpson, 1998; Eriksson et al., 1998). Furthermore, prolonged periods of precipitation allied with an absence of soil-forming processes and a lack of binding mineral cements would facilitate the rapid infiltration of surface water, thereby potentially contributing to a rapid rate of rise of the local water table in the aftermath of fluvial flood events (Tirsgaard and Øxnevad, 1998; Al-Masrahy and Mountney, 2015).

The wet aeolian systems represented by the lower deposits in each preserved depositional cycle were succeeded by a largely dry aeolian system represented by the overlying deposits. These aeolian systems developed in a context where the water table lay beneath the accumulation surface, leaving dry sediments potentially available for aeolian transport, given an appropriate aerodynamic configuration (Kocurek and Havholm, 1993). Accumulation in a dry aeolian system requires a positive net sediment budget. Conditions that favour dry aeolian system accumulation are as follows: (i) the generation of a sediment supply that is available for aeolian transport; (ii) a downstream decrease in the transport rate, and/or decrease in sediment concentration over time such that sand saturation (i.e., complete cover) of the substrate ensues whereby aeolian dunes grow to cover the entire accumulation surface at the expense of adjacent interdune flats; and (iii) the onset of climbing of migrating aeolian dunes over one another at a positive angle leading to accumulation. At times when conditions become favorable for the accumulation of a dry aeolian system, aeolian construction, accumulation, bypass and deflation are controlled exclusively by aerodynamic behaviour of the flow (Kocurek and Havholm, 1993; Scherer and Lavina, 2005; Kocurek and Ewing, 2012).

The occurrence of depositional cycles, which internally comprise a predictable vertical order of facies and which are each of a similar thickness and themselves stacked vertically, suggests that allogenic factors controlled the accumulation of each cycle and the repeated development of each successive cycle (Fig. 7). Within each cycle, the repeated occurrence of interdune deposits with adhesion-ripple strata and possible MISS indicates that the water table episodically intercepted the accumulation surface. Such deposits are evidence of the development of small, ephemeral ponds in the spatially confined interdune depressions between the aeolian dunes.

In many sections, the occurrence of small-scale sets of cross-strata is replaced upward by medium- to large-scale sets, many examples of which lack associated interdune elements. This could reflect either a temporal increase in aeolian bed form size or in angle of climb (Kocurek and Havholm, 1993; Mountney, 2006). Both of these conditions could result from an increase in the availability of sand for aeolian transport and bedform construction leading to accumulation.

The widespread occurrence of aeolian dune sets dominated by grainflow strata indicative of well-developed slipfaces that passed downslope into wind-ripple dominated dune plinth areas allied with the dominantly unimodal dip to the NNE of foreset azimuths is typical of simple crescentic dunes migrating under persistent unimodal winds that blew to the north-northeast. The absence of large-scale draas deposits could suggest accumulation in a setting close to the erg margin, where the sediment supply was likely insufficient to construct the very large bedforms, or it could alternatively indicate that the studied aeolian succession represents an erg system for which the supply of sand was limited.

Each preserved aeolian depositional cycle is bounded by a laterally extensive, continuous, non-climbing surface that truncates underlying sets of dune strata in an erosional contact. These are deflationary supersurfaces (Loope, 1985; Kocurek and Havholm, 1993) and each represents the termination of an episode of erg accumulation. Their occurrence at the top of each cycle throughout the succession demonstrates that the formation comprises at least 14 separate sequences. Each supersurface records a hiatus in accumulation (Blakey and Middleton, 1983; Loope, 1985; Talbot, 1985). The genesis of the supersurfaces requires a negative sediment budget, where an earlier accumulation is susceptible to erosion. Exhaustion of an upwind sand supply is the most likely cause of the onset of supersurface development in dry aeolian systems. The successive drying-upward cycles and the nature of the deposits indicate distinct and repeated episodes of aeolian accumulation. The planar and horizontal geometry of the supersurfaces indicates deflation whereby part of the previous, underlying genetic unit was subject to erosion. The absence of a granule or pebble deflation lag associated with the supersurfaces indicates the erosion of aeolian dune sediments (fine to medium sand). The absence of the features related to surfaces created by scour to a near surface groundwater-table (e.g., evaporite cements, erosional relief) indicates that deflation occurred only to a level above the water table (Kocurek et al., 1991b; Havholm and Kocurek, 1994).

8. Discussion

The Mangabeira Formation of the São Francisco Craton records multiple cycles of aeolian accumulation and deflation related expressed as at least 14 drying-upward cycles (Fig. 7). The shift between periods of accumulation and deflation in aeolian system may occur as a result of change in eustasy, tectonic and climate cycles (Kocurek, 1998). There is no evidence for the activity of marine processes in influencing aeolian system construction, accumulation and preservation in the Lower Unit of the Mangabeira Formation. Tectonic activity determined aeolian system accumulation, via its role in driving the basin subsidence responsible for generating accommodation and by enabling preservation of the sedimentary succession via a net long-term relative rise in the water table level. Previous studies (Schobbenhaus and Kaul, 1971; Alkmim and Martins-Neto, 2011) show that the Mangabeira Formation deposits were deposited in a sag basin that developed as the end-product of a phase of Palaeoproterozoic rifting. Such sag basins are characterized by thermal-flexure subsidence; local tectonic movements did not apparently influence the high-frequency oscillations of the palaeo-water table level (Blakey, 1988; Veiga et al., 2002). In consequence of this, the main controlling factor that principally influenced episodes of aeolian system accumulation and deflation was climate change. Repeated shifts between arid and humid climatic phases changed both the aeolian sediment budget and the level of the water table in the basin (Fig. 7). These factors themselves influenced governed how the erg sequences accumulated and became preserved.

Onset of episodes of aeolian system accumulation occurred during a humid climate phase, as demonstrated by aeolian sandsheet deposits, adhesion strata and minor waterlain deposits all indicative of a wet aeolian system. In wet aeolian systems, a near-surface water table controls accumulation (Kocurek and Havholm, 1993). During humid episodes, the availability of sand for aeolian transport is limited since much of the surface is damp due to the relatively high, near-surface water table (Kocurek, 1999). Increased precipitation also increases fluvial run off into the aeolian system, thereby driving local water-table rise, further reducing the availability of sand for aeolian transport. Such processes inhibit aeolian dune construction, instead favouring aeolian sandsheet development (Kocurek and Nielson, 1986). The intercalation of adhesion structures and the microbially induced lamination with wind-ripple lamination within an aeolian sandsheet facies may indicate fluctuating ground water table in response to low-magnitude flood events (Chakraborty and Chaudhuri, 1993) or "freezing" of ripples by rising capillary moisture (Kocurek and Nielson, 1986).

As the climate became increasingly arid, the aeolian system changed. Each preserved cycle became dominated by dry aeolian sandsheet deposition. These dry sandsheets were characterized by wind-ripple strata and small aeolian dunes. In this pre-vegetation system, sediment would have been more readily available for aeolian transport, even in semi-arid climates, given the absence of the substrate-binding effects of vegetation. As the relative water table fell in response to increased aridity, large volumes of stored (time-lagged) supplies of sediment would have become available for aeolian transport (Simpson and Eriksson, 1993; Trewin, 1993; Kocurek and Lancaster, 1999). With increasing aridity, the aeolian sandsheet deposits were replaced by climbing aeolian dune systems within a sand sea (erg), thereby establishing the dry aeolian system. In dry aeolian systems, the water table and its capillary fringe are far below the depositional surface. Therefore aeolian deposition, bypass and erosion are entirely controlled by aerodynamic conditions of the flow (Kocurek and Havholm, 1993). The accumulation of aeolian dunes commenced when the angle of climb became positive. The development of crescentic dunes is associated with, limited yet continuous, sand availability (Mckee, 1979). The unimodal wind regime was punctuated by annual fluctuations, as revealed by the presence of multiple reactivation surfaces identified in the aeolian dune strata. The local occurrence of lenses of damp interdune deposits between aeolian dunes indicates an oscillation in the ground-water table, with or without a variable angles of bedform climbing (Mountney and Thompson, 2002; Mountney, 2012).

The climax of aeolian system accumulation was signalled by a change from accumulation to deflation. The development of deflationary supersurfaces commonly results from an external change forced on the system (Havholm and Kocurek, 1994). Most aeolian systems have a finite sediment supply that is used for their construction and accumulation. Much of that supply is made available during the transition from humid to arid climatic episodes when the water table is low. In response to a protracted episode of aridity, the aeolian sand supply was eventually depleted, leading to the onset of aeolian bedform cannibalization and deflation via a change from a positive to a negative angle of bedform climb, culminating in the generation of a deflationary supersurface (Loope, 1985; Mountney, 2006, 2012).

9. Conclusions

Although several aeolian erg successions of Proterozoic age have been described previously (see Rodríguez-López, 2014 and references therein), and some have been the subject of facies analysis for the purpose of reconstruction of palaeoenvironment (Deynoux et al., 1989; Chakraborty, 1991; Simpson and Eriksson, 1993; Biswas, 2005; Basu et al., 2014), the aeolian succession of the Mangabeira Formation represents the only detailed study of a Proterozoic erg succession for which a well-defined sedimentary cyclicity has been attributed to successive drying-upward cycles. The thickness and vertical facies successions are similar to drying-upward cycles widely described in Phanerozoic successions (e.g. Yang and Nio, 1993; George and Berry, 1993; Clemmensen *et al.,* 1994; Howell and Mountney, 1997; Veiga *et al.*, 2002; Mountney 2006), which indicate similar conditions of aeolian construction, accumulation and preservation.

In the lower Mangabeira Formation, 14 drying-upward cycles record distinct episodes of sediment accumulation, and establishment and accumulation of distinct dune fields. Episodes of aeolian accumulation were followed by partial deflation whereby a deflationary supersurface defines the top of each depositional cycle. Four distinct facies associations are identified in the deposits of the drying-upward cycles: aeolian sandsheet and waterlain deposits pass upward into aeolian dune and interdune deposits. The lower and upper parts of each cycle accumulated as wet and dry aeolian systems, respectively. The wet aeolian systems accumulated under the influence of a near-surface water table. The occurrence of wind-ripple strata, adhesion structures and water-lain deposits characterized these systems. Small-scale fluctuations in lithofacies arrangements within these deposits indicate repeated episodes of water-table rise and fall relative to the accumulation surface over time. The dry aeolian systems accumulated in a setting where the water table and its capillary fringe were continuously beneath the level of the accumulation surface. In such systems, sediment is potentially available for aeolian transport, given an appropriate aerodynamic configuration.

The nature of the genetic units and the supersurfaces that bound the cycles indicates multiple hiatuses in accumulation and repeated partial deflation of parts of the succession, likely in response to climatic changes. The depositional architecture of the preserved sequences was determined by the complex interaction of water-table fluctuations, the generation of a sediment supply, the availability of that sediment for aeolian system construction, and changes in the transport capacity of the wind.

Acknowledgements

This research was completed as part of the doctoral project carried out by the first author. We are grateful to the institutions Petrobras and National Council for Scientific and Technological Development (CNPq) for their provision of direct or indirect support. We thank the Editor Jasper Knight, and reviewers Tapan Chakraborty, Luis Spalletti and an anonymous reviewer for helpful comments that led to considerable improvement of the manuscript.

References

Almeida, F.F.M., 1977. O Cráton do São Francisco. Revista Brasileira de Geociências 7, 349–364.

Alkmim, F.F., Martins-Neto, M.A., 2012. Proterozoic first-order sedimentary sequences of the São Francisco craton, eastern Brazil. Marine and Petroleum Geology 33, 127–139.

Al-Masrahy, M.A., Mountney, N.P., 2015. A classification scheme for fluvial–aeolian system interaction in desert-margin settings. Aeolian Research 17, 67–88.

Babinski, M., Pedreira, A.J., Brito Neves, B.B., Van Schmus, W.R., 1999. Contribuição à geocronologia da Chapada Diamantina. In: Pedreira, A.J. (Ed.), VII Simpósio Nacional de Estudos Tectônicos. Brazilian Geological Society, pp. 118–120.

Barbosa, J., Martin, H., Peucat, J.J., 2004. Palaeoproterozoic dome-forming structures related to granulite-facies metamorphism, Jequié block, Bahia, Brazil: petrogenetic approaches. Precambrian Research 135, 105–131.

Basu, H., Sastry, R.S., Achar, K.K., Umamaheswar, K., Parihar, P.S., 2014. Palaeoproterozoic fluvio-aeolian deposits from the lower Gulcheru Formation, Cuddapah Basin, India. Precambrian Research 246, 321–333.

Biswas, A. S., 2005. Coarse aeolianites: sand sheets and zibar-interzibar facies from the Mesoproterozoic Cuddapah Basin, India. Sedimentary Geology 174, 149–160.

Blakey, R.C., 1988. Basin tectonics and erg response. Sedimentary Geology 56, 127–151.

Blakey, R.C., Middleton, L.T., 1983. Permian Shoreline Eolian Complex in Central Arizona: Dune Changes in Response to Cyclic Sealevel Changes. In: Brookfield, M.E., Ahlbrandt, T.S. (Eds.), Eolian Sediments and Processes, Developments in Sedimentology 38. Elsevier, New York, pp. 551–581.

Bose, P.K., Eriksson, P.G., Sarkar, S., Wright, D.T., Samanta, P., Mukhopadhyay, S., Mandal, S., Banerjee, S., Altermann, W., 2012. Sedimentation patterns during the Precambrian: A unique record? Marine and Petroleum Geology 33, 34–68.

Brookfield, M.E., 1977. The origin of bounding surfaces in ancient aeolian sandstones. Sedimentology 24, 303–332.

Cain, S., Mountney, N.P., 2011. Downstream changes and associated fluvial-eolian interactions in an ancient terminal fluvial system: the Permian Organ Rock Formation, SE Utah, U.S.A. In: Davidson, S., Leleu, S., North, C. (Eds.), From River to Rock Record, SEPM Special Publication 97, pp. 167–185.

Chakraborty, T., 1991. Sedimentology of a Proterozoic erg: the Venkarpur Sandstone, Pranhita-Godavari Valley, south India. Sedimentology 38, 301–322.

Chakraborty, T., Chaudhuri, A. K., 1993. Fluvial-aeolian interactions in a Proterozoic alluvial plain: example from the Mancheral Quartzite, Sullavai Group, Pranhita-Godavari Valley, India. In: Pye, K. (Ed.), The Dynamics and Environmental Context of Aeolian Sedimentary Systems. Geological Society of London, London, Special Publications 72, pp. 127–141.

Chemale, F., Dussin, I.A., Alkmim, F.F., Sousa, M., Queiroga, G., Armstrong, R., Santos, M.N., 2012. Unravelling a Proterozoic basin history through detrital zircon geochronology: The case of the Espinhaço Supergroup, Minas Gerais, Brazil. Gondwana Research 22, 200–206.

Clemmensen, L.B., Olsen, H., Blakey, R.C., 1989. Erg-margin deposits in the Lower Jurassic Moenave Formation and Wingate Sandstone, southern Utah. Geological Society of America Bulletin 101, 759–773.

Clemmensen, L.B., Hegner, J., 1991. Eolian sequence and erg dynamics: the Permian Corrie Sandstone, Scotland. Journal of Sedimentary Petrology 61, 768–774.

Clemmensen, L.B., Oxnevad, I.E.I., Boer, P.L., 1994. Climatic control on ancient desert sedimentation: some Paleozoic and Mesozoic examples from NW Europe and western interior of USA. In: Boer, D.L., Smith, D.E. (Eds.), Orbital Forcing and Cyclic Sequences. IAS Special Publication 19, pp. 19–29.

Cruz, S.C.P., Alkmim, F.F., 2006. The tectonic interaction between the Paramirim Aulacogen and the Araçuaí Belt, São Francisco Craton region, Eastern Brazil. Anais da Acadêmia Brasileira de Ciências 78, 151–173.

Danderfer, A., De Waele, B., Pedreira, A.J., Nalini, H. A., 2009. New geochronological constraints on the geological evolution of Espinhaço basin within the São Francisco Craton-Brazil. Precambrian Research 170, 116–128.

Deynoux, M., Kocurek, G., Proust, J.N., 1989. Late Proterozoic periglacial aeolian deposits on the West African Platform, Taoudeni Basin, western Mali.

Sedimentology 36, 531–549.

Eriksson, K.A., Simpson, E.L., 1998. Controls on spatial and temporal distributions of Precambrian eolianites. Sedimentary Geology 120, 275–294.

Eriksson, P.G., Condie, K.C., Tirsgaard, H., Mueller, W.U., Altermann, W., Miall, A. D., Aspler, L.B., Catuneanu, O., Chiarenzelli, J.R., 1998. Precambrian clastic sedimentation systems. Sedimentary Geology 120, 5–53.

Eriksson, P.G., Simpson, E.L., Eriksson, K.A., Bumby, A.J., Steyn, G.L., Sarkar, S., 2000. Muddy Roll-up Structures in Siliciclastic Interdune Beds of the c. 1.8 Ga Waterberg Group, South Africa. Palaios 15, 177–183.

Fryberger, S.G., Schenk, C.J., Krystinik, L.F., 1988. Stokes surfaces and effects of near-surface groundwater-table on aeolian deposition. Sedimentology 35, 21–41.

George, G.T., Berry, J.K., 1993. A new lithostratigraphy and depositional model for the Upper Rotliegend of the UK sector of the Southern North Sea. In: North, C.P., Prosser, D.J. (Eds.), Characterization of fluvial and aeolian Reservoirs. Geological Society of London, Special Publications 73, pp. 291-320.

Grotzinger, J.P., Arvidson, R.E., Bell, J.F., Calvin, W., Clark, B.C., Fike, D.A., Golombek, M., Greeley, R., Haldemann, A., Herkenhoff, K.E., Jolliff, B.L., Knoll, A.H., Malin, M., McLennan, S.M., Parker, T., Soderblom, L., Sohl-Dickstein, J.N., Squyres, S.W., Tosca, N.J., Watters, W.A., 2005. Stratigraphy and sedimentology of a dry to wet eolian depositional system, Burns formation, Meridiani Planum, Mars. Earth and Planetary Science Letters 240, 11-72.

Guadagnin, F., Chemale, F., Magalhães, A.J.C., Alessandretti, L., Bállico, M.B., Jelinek, A.R., 2015a. Sedimentary petrology and detrital zircon U – Pb and Lu – Hf constraints of Mesoproterozoic intracratonic sequences in the Espinhaço Supergroup : Implications for the Archean and Proterozoic evolution of the São Francisco Craton. Precambrian Research 266, 227–245.

Guadagnin, F., Chemale, F., Magalhães, A.J.C., Santana, A., Dussin, I.A., Takehara, L., 2015b. Age constraints on crystal-tuff from the Espinhaço Supergroup - Insight into the Paleoproterozoic to Mesoproterozoic intracratonic basin cycles of the Congo-São Francisco Craton. Gondwana Research 27, 363–376.

Guimarães, J.T., Santos, R.A., Melo, R.C., 2008. Geologia da Chapada Diamantina Ocidental (Projeto Ibitiara - Rio de Contas). Salvador, Companhia Baiana de Pesquisa Mineral - CPRM. Série Arquivos Abertos 31, 64p.

Hayes, A.G., Grotzinger, J.P., Edgar, L.A., Squyres, S.W., Watters, W.A., Sohl-Dickstein, J., 2011. Reconstruction of eolian bed forms and paleocurrents from cross-bedded strata at Victoria Crater, Meridiani Planum, Mars. Journal of Geophysical Research 116, E00F21, DOI: 10.1029/2010JE003688.

Havholm, K., Kocurek, G., 1994. Factors controlling aeolian sequence stratigraphy: clues from super bounding surface features in the Middle Jurassic Page Sandstone. Sedimentology 41, 913–934.

Heness, E.A., Simpson, E.L., Bumby, A.J., Eriksson, P.G., Eriksson, K.A., Hilbert-Wolf, H.L., Okafor, O.J., Linnevelt, S., Fitzgerald Malenda, H., Modungwa, T., 2014. Evidence for climate shifts in the ~2.0 Ga Upper Makgabeng Formation erg, South Africa. Palaeogeogrraphy, Palaeoclimatology, Palaeoecolology 409, 265–279.

Howell, J.A., Mountney, N.P., 1997. Climatic cyclicity and accommodation space in arid to semi-arid depositional systems: an example from the Rotliegend Group of the Southern North Sea. In: Zielger, K., Turner, P., Dalnes, S.R. (Eds.), Petroleum Geology of the Southern North Sea: Future Potential. Geological Society of London, Special Publications 123, pp. 63-86.

Hunter, R.E., 1977. Basic types of stratification in small eolian dunes. Sedimentology 24, 361–387.

Hunter, R.E., Rubin, D.M., 1983. Interpreting cyclic crossbedding, with an example from the Navajo Sandstone. In: Brookfield, M.E., Ahlbrandt, T.S. (Eds.), Eolian Sediments and Processes, Developments in Sedimentology 38. Elsevier, New York, pp. 429–454.

Jackson, M.J., Simpson, E.L., Eriksson, K.A., 1990. Facies and sequence stratigraphic analysis in an intracratonic, thermal-relaxation basin: the Early Proterozoic, Lower Quilalar Formation and Ballara Quartzite, Mount Isa Inlier, Australia. Sedimentology 37, 1053–1078.

Kocurek, G., 1981. Significance of interdune deposits and bounding surfaces in aeolian dune sands. Sedimentology 28, 753–780.

Kocurek, G., Fielder, G., 1982. Adhesion structures. Journal of Sedimentary Research 52, 1229–1241.

Kocurek, G., Hunter, R.E., 1986. Origin of polygonal fractures in sand, uppermost Navajo and Page sandstones, Page, Arizona. Journal of Sedimentary Research 56, 895–904.

Kocurek, G., Nielson, J., 1986. Conditions favourable for the formation of warm-climate aeolian sand sheets. Sedimentology 33, 795–816.

Kocurek, G., 1988. First-order and super bounding surfaces in eolian sequences—Bounding surfaces revisited. Sedimentary Geology 56, 193–206.

Kocurek, G., Havholm, K., Deynoux, M., Blakey, R.C., 1991a. Amalgamated accumulations resulting from climatic and eustatic changes, Akchar Erg, Mauritania. Sedimentology 38, 751–772

Kocurek, G., Knight, J., Havholm, K., 1991b. Outcrop and semi-regional three-dimensional architecture and reconstruction of a portion of the eolian Page Sandstone (Jurassic). In: Miall, A.D., Tyler, N. (Eds.), The three-dimensional facies architecture of terrigenous clastic sediments and its implications for hydrocarbon discovery and recovery. SEPM, Concepts in Sedimentology and Paleontology 3, pp. 25-43.

Kocurek, G., Havholm, K.G., 1993. Eolian sequence stratigraphy - A conceptual framework. In: Weimer, P., Posamentier, H. (Eds.), Siliclastic Sequence Stratigraphy, AAPG Memoir 58, Tulsa, pp. 393-409.

Kocurek, G., 1996. Desert aeolian systems. In: Reading, H.G. (Ed.), Sedimentary

Environments: Processes, Facies and Stratigraphy. Blackwell, Oxford, UK, pp. 125–153.

Kocurek, G., 1998. Aeolian system response to external forcing factors - a sequence stratigraphic view of the Saharan region. In: Alsharhan, A.S., Glennie, K., Whittle, G.L., Kendall, C.G.St.C. (Eds.), Quaternary Deserts and Climatic Change. Rotterdam, Balkema, pp. 327-337.

Kocurek, G., 1999. The Aeolian Rock Record (Yes, Virginia, it Exists, But it Really is Rather Special to Create One). In: Goudie, A.S., Livingstone, I., Stokes, S. (Eds.), Aeolian Environments, Sediments and Landforms. John Wiley and Sons Ltd, Chichester, pp. 239–259.

Kocurek, G., Lancaster, N., 1999. Aeolian system sediment state: Theory and Mojave Desert Kelso dune field example. Sedimentology 46, 505–515.

Kocurek, G., Ewing, R.C., 2012. Source-To-Sink: an earth/mars comparison of boundary conditions for eolian dune systems. In: Grotzinger, J.P., Milliken, R.E. (Eds.), Sedimentary Geology of Mars, SEPM Special Publication 102, pp. 151–168.

Lancaster, N., 1992. Relations between dune generations in the Gran Desierto of Mexico. Sedimentology 39, 631–644.

Langford, R.P., Chan, M.A., 1988. Flood surfaces and deflation surfaces within the Cutler Formation and Cedar Mesa Sandstone (Permian), southeastern Utah. Bulletin of Geological Society of America 100, 1541–1549.

Langford, R.P., Chan, M.A., 1989. Fluvial-aeolian interactions: Part II, ancient systems. Sedimentology 36, 1037–1051.

Loope, D.B., 1985. Episodic deposition and preservation of eolian sands: a late Paleozoic example from southeastern Utah (Canyonlands National Park, USA). Geology 13, 73–76.

Mckee, E.D., 1979. A Study of Global Sand Seas. Geological Survey Professional Paper 1052, Washington.

Miall, A.D., 1977. A review of the braided-river depositional environment. Earth-Science Reviews 13, 1–62.

Miall, A.D., 2006. The Geology of Fluvial Deposits, 4th ed. Springer-Verlag, Berlin.

Mountney, N.P., Howell, J., Flint, S., Jerram, D., 1999. Climate, sediment supply and tectonics as controls on the deposition and preservation of the aeolian-fluvial Etjo Sandstone Formation, Namibia. Journal o Geological Society of London 156, 771–777.

Mountney, N.P., Thompson, D.B., 2002. Stratigraphic evolution and preservation of aeolian dune and damp/wet interdune strata: An example from the Triassic Helsby Sandstone Formation, Cheshire Basin, UK. Sedimentology 49, 805–833.

Mountney, N.P., Jagger, A., 2004. Stratigraphic evolution of an aeolian erg margin system: The Permian Cedar Mesa Sandstone, SE Utah, USA. Sedimentology 51, 713–743.

Mountney, N.P., 2006. Periodic accumulation and destruction of aeolian erg sequences in the Permian Cedar Mesa Sandstone, White Canyon, southern Utah, USA. Sedimentology 53, 789–823.

Mountney, N.P., 2012. A stratigraphic model to account for complexity in aeolian dune and interdune successions. Sedimentology 59, 964–989.

Noffke, N., 2010. Geobiology: Microbial mats in sandy deposits from the archean era to today. Springer, Heidelberg.

Owen, G., 2003. Load structures: gravity-driven sediment mobilization in the shallow subsurface. In: Van Rensbergen, P., Hillis, R.R., Maltman, A.J., Morley, C.K. (Eds.), Subsurface Sediment Mobilization. Geological Society of London, Special Publications 216, pp. 21–34.

Paim, P.S.G., Scherer, C.M.S., 2007. High-resolution stratigraphy and depositional model of wind- and water-laid deposits in the ordovician Guaritas rift (Southernmost Brazil). Sedimentary Geology 202, 776–795.

Pedreira, A.J., 1994. O supergrupo Espinhaço na Chapada Diamantina Centro -

Oriental, Bahia: sedimentologia, estratigrafia e tectônica. Ph.D. Thesis, Universidade de São Paulo, Brasil.

Pedreira, A.J., de Waele, B., 2008. Contemporaneous evolution of the Palaeoproterozoic-Mesoproterozoic sedimentary basins of the São Francisco-Congo Craton. In: Pankhurst, R.J., Trouw, R.A.J., Brito Neves, B.B., De Wit, M.J. (Eds.), West Gondwana: Pre-Cenozoic Correlations Across the South Atlantic Region. Geological Society, London, Special Publications 294, pp. 33–48.

Rodríguez-López, J.P., Meléndez, N., De Boer, P.L., Soria, A.R., 2008. Aeolian sand sea development along the mid-Cretaceous western Tethyan margin (Spain): Erg sedimentology and palaeoclimate implications. Sedimentology 55, 1253–1292.

Rodríguez-López, J.P., Clemmensen, L.B., Lancaster, N., Mountney, N.P., Veiga, G.D., 2014. Archean to Recent aeolian sand systems and their sedimentary record: Current understanding and future prospects. Sedimentology 61, 1487-1534.

Ross, G.M., 1983. Bigbear Erg: A Proterozoic Intermontane Eolian Sand Sea in the Hornby Bay Group, Northwest Territories, Canada. In: Brookfield, M.E., Ahlbrandt, T.S. (Eds.), Eolian Sediments and Processes, Developments in Sedimentology 38. Elsevier, New York, pp. 483–519.

Rubin, D., Hunter, R., 1982. Bedform climbing in theory and nature. Sedimentology 29, 121–138.

Rubin, D.M., 1987. Formation of scalloped cross-bedding without unsteady flows. Journal of Sedimentary Research 57, 39–45.

Santos, M.N., Chemale, F., Dussin, I.A., Martins, M., Assis, T.A.R., Jelinek, A.R., Guadagnin, F., Armstrong, R., 2013. Sedimentological and paleoenvironmental constraints of the Statherian and Stenian Espinhaç rift system, Brazil. Sedimentary Geology 290, 47–59.

Sarkar, S., Bose, P.K., Samanta, P., Sengupta, P., Eriksson, P.G., 2008. Microbial mat mediated structures in the Ediacaran Sonia Sandstone, Rajasthan, India, and their implications for proterozoic sedimentation. Precambrian Research 162, 248–263.

Scherer, C.M.S., 2000. Eolian dunes of the Botucatu Formation (Cretaceous) in southernmost Brazil: Morphology and origin. Sedimentary Geology 137, 63–84.

Scherer, C.M.S., Lavina, E.L.C., 2005. Sedimentary cycles and facies architecture of aeolian-fluvial strata of the Upper Jurassic Guará Formation, southern Brazil. Sedimentology 52, 1323–1341.

Schobbenhaus, C., Hoppe, A., Baummann, A., Lork, A., 1994. Idade U/Pb do vulcanismo Rio dos Remédios Chapada Diamantina, Bahia. 38º Congresso Brasileiro de Geologia, Resumos Expandidos, Sociedade Brasileira de Geologia, pp. 397–398.

Schobbenhaus, C., Kaul, P.F.T., 1971. Contribuição a estratigrafia da Chapada Diamantina, Bahia Central. Mineração e Metalurgia 53, 116–120.

Silveira, E.M., Söderlund, U., Oliveira, E.P., Ernst, R.E., Leal, A.B.M., 2013. First precise U-Pb baddeleyite ages of 1500Ma mafic dykes from the São Francisco Craton, Brazil, and tectonic implications. Lithos 174, 144–156.

Simpson, E.L., Eriksson, K.A., 1993. Thin eolianites interbedded within a fluvial and marine succession: Early Proterozoic Whitworth Formation, Mount Isa Inlier, Australia. Sedimentary Geology 87, 39–62.

Souza, E.G., 2012. Arquitetura de fácies e evolução estratigráfica dos depósitos eólicos da Formação Mangabeira, Supergrupo Espinhaço - BA. Monography Thesis, Universidade Federal do Rio Grande do Sul, Brasil.

Sullivan, R., Banfield, D., Bell, J.F., Calvin, W., Fike, D., Golombek, M., Greeley, R., Grotzinger, J., Herkenhoff, K., Jerolmack, D., Malin, M., Ming, D., Soderblom, L.A., Squyres, S.W., Thompson, S., Watters, W.A., Weitz, C.M., Yen, A., 2005. Aeolian processes at the Mars Exploration Rover Meridiani Planum landing site, Nature 436, 58 – 61.

Talbot, M.R., 1985. Major bounding surfaces in aeolian sandstones-a climatic model. Sedimentology 32, 257–265.

Tirsgaard, H., Øxnevad, I.E.I., 1998. Preservation of pre-vegetational mixed fluvio-aeolian deposits in a humid climatic setting: an example from the Middle Proterozoic Eriksfjord Formation, Southwest Greenland. Sedimentary Geology 120, 295–317.

Trewin, N.H., 1993. Controls on fluvial deposition in mixed fluvial and aeolian facies within the Tumblagooda Sandstone (Late Silurian) of Western Australia. Sedimentary Geology 85, 387–400.

Veiga, G.D., Spalletti, L.A., Flint, S., 2002. Aeolian / fluvial interactions and high-resolution sequence stratigraphy of a non-marine lowstand wedge: the Avilé Member of the Agrio Formation (Lower Cretaceous), central Neuquén Basin, Argentina. Sedimentology 49, 1001–1019.

Yang, C.S., Nio, S.D., 1993. Application of highresolution sequence stratigraphy to the Upper Rotliegend in the Netherlands offshore. In: Weimer, P., Posamentier, H.W. (Eds.), Siliciclastic sequence stratigraphy - Recent developments and applications. American Association of Petroleum Geologists Memoir 58, pp. 285-316.

Figure Captions

Fig. 1. (A) Location of the São Francisco craton (in black). Position of the Chapada Diamantina Range indicated by white square. (B) Simplified geological map of the Chapada Diamantina Range, based on Geological Survey of Brazil (CPRM). The yellow colour represents the Mangabeira Formation. The area selected for detailed study is in a non-deformed part of the Chapada Diamantina Range (black square). (C) Localities 1 to 11 represent measured sedimentological sections.

Fig. 2. Schematic stratigraphic section of the Espinhaço Supergroup at the Chapada Diamantina Range. Ages from Guadagnin et al. (2015b). The relationship between sedimentary units, depositional environments and tectonic settings are indicated.

Fig. 3. Measured sedimentological sections and schematic cross-section showing the regional dip-azimuth and the main facies associations and sedimentary structures. The rose diagram shows all the foreset dip-azimuth readings. Red arrow indicates the mean orientation.

Fig. 4. The main sedimentary structures on aeolian dunes facies association. (A) Intertonguing relationship between grain flow laminae (gf), each 10 to 80 mm thick and sub-critically climbing translatent strata (wr) with 5 to 10 mm thick. (B) Stacked wind-ripple lamination. (C) Wind-parallel section shows aeolian dunes with interdune surfaces (I) which separate simple cross-sets. Some sets exhibit reactivation surfaces (R). Dune migration direction was from left to right.

Fig. 5. The main sedimentary structures of aeolian interdunes facies association. (A) External geometry of interdunes deposits. Note irregular contact suggesting interdune hollow or corridors between aeolian dunes. Wind-oblique section. (B) 10 to 20 cm thick unit of damp interdune deposits preserved between aeolian dunes deposits. (C) Dry interdune with millimetric, inversely graded, horizontal lamination (wr). (D) Dry to damp interdune with wind-ripple lamination (wr) and adhesion lamination (ar). (E) Very fine- to fine-grained sandstone alternating with millimetric irregular mudstone laminae; exhibits wavy and crinkly lamination (adhesion structures - ar).

Fig. 6. The main sedimentary structures of aeolian sandsheets and fluvial deposits. (A) Millimetric, inverse graded, horizontally to low-angle translatent lamination in aeolian sandsheets deposits. Lamination exhibits weak inverse grain-size grading. (B) Isolated aeolian dune between sandsheet deposits. Thickness of the bed is 20 cm. (C) Millimetric to centimetric sandstones with crinkly lamination. (D) and (E) Centimetric subaqueous ripple lamination of fluvial origin. (F) Small-scale load-cast structures (lc) interlayered with adhesion structures (ar).

Fig. 7. Relationship between water-table oscillations, depositional surfaces and facies associations observed in the Lower Unit of the Mangabeira Formation. The alternation between wet and dry aeolian systems, and the development of supersurfaces. The

succession records high-frequency changes of the water table, sediment supply, sediment availability and wind transport capacity caused by oscillating climate changes.

Fig. 8. Interpretation of outcrop panel and correlation with the GPR line showing the relationship between facies association and supersurfaces. The GPR line was acquired along a roadside section directly in front of the outcrop.

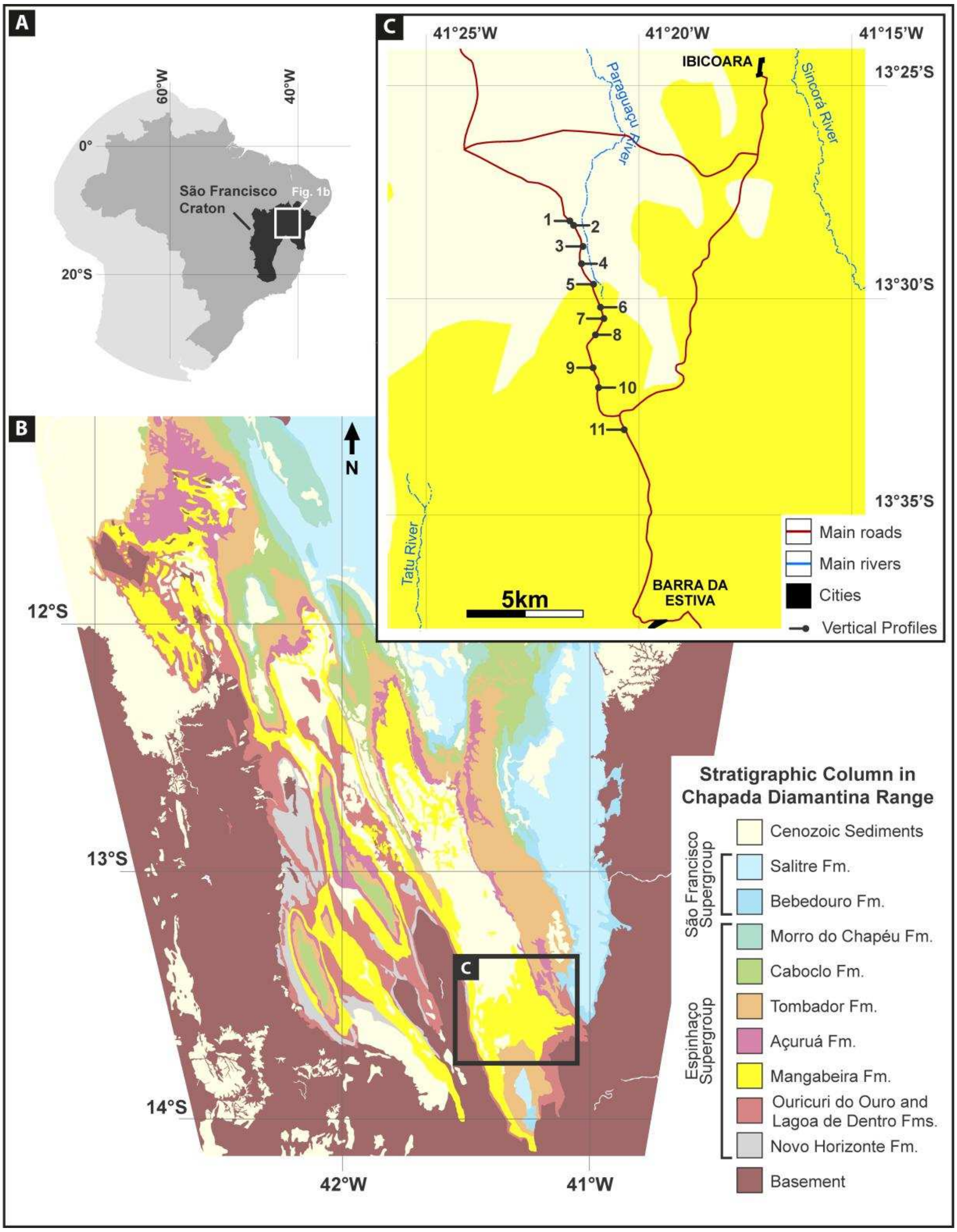
A
60°W
40°W
0°
São Francisco
Craton
Fig. 1b
20°S
C
41°25'W
41°20'W
41°15'W
IBICOARA
13°25'S
Paraguaçu River
Sincorá River
13°30'S
1
2
3
4
5
6
7
8
9
10
11
13°35'S
Tatu River
5km
BARRA DA
ESTIVA
Main roads
Main rivers
Cities
Vertical Profiles
B
N
12°S
13°S
14°S
42°W
41°W
C
Stratigraphic Column in
Chapada Diamantina Range
Cenozoic Sediments
São Francisco
Supergroup
Salitre Fm.
Bebedouro Fm.
Espinhaço
Supergroup
Morro do Chapéu Fm.
Caboclo Fm.
Tombador Fm.
Açuruá Fm.
Mangabeira Fm.
Ouricuri do Ouro and
Lagoa de Dentro Fms.
Novo Horizonte Fm.
Basement

Figure 1

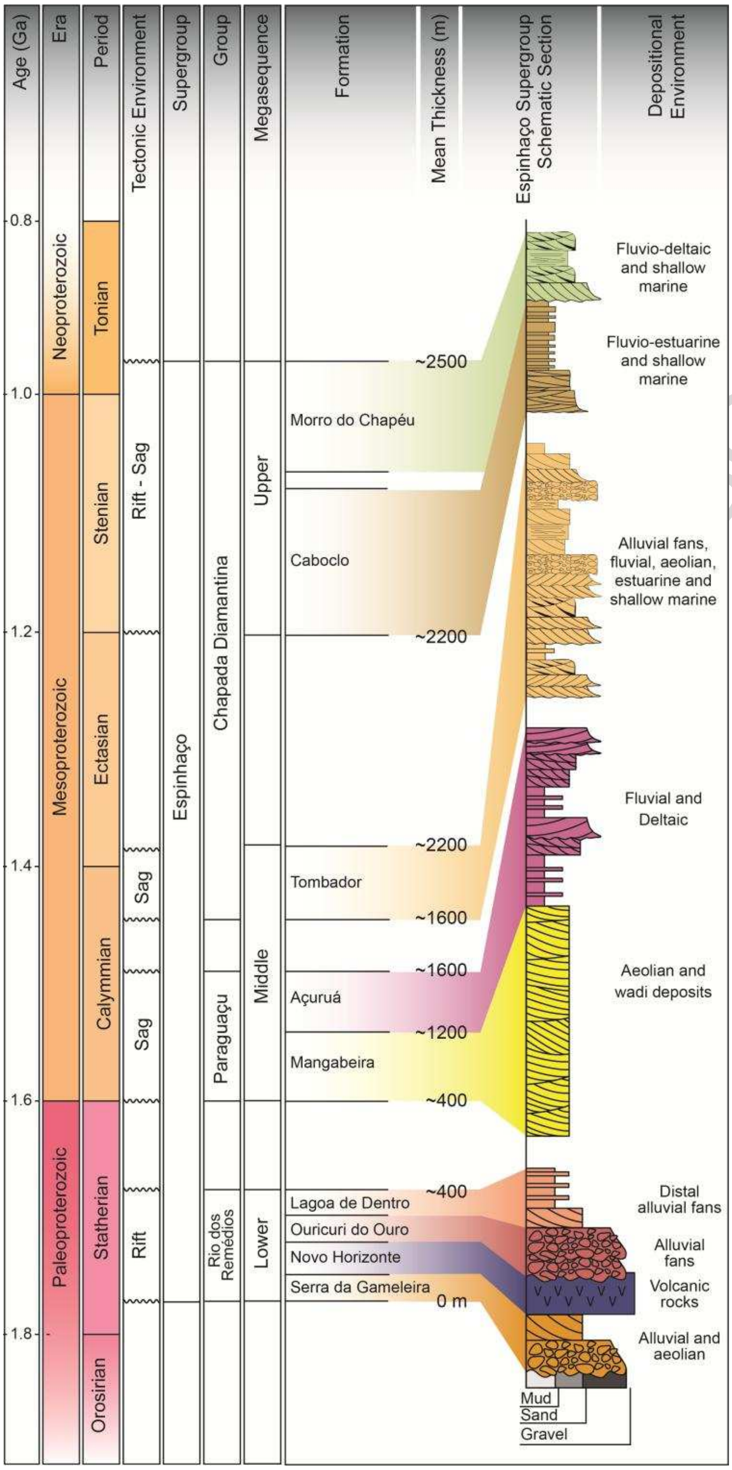
Age (Ga)
Era
Period
Tectonic Environment
Supergroup
Group
Megasequence
Formation
Mean Thickness (m)
Espinhaço Supergroup Schematic Section
Depositional Environment
0.8
1.0
1.2
1.4
1.6
1.8
Neoproterozoic
Mesoproterozoic
Paleoproterozoic
Tonian
Stenian
Ectasian
Calymmian
Statherian
Orosirian
Rift - Sag
Sag
Sag
Rift
Espinhaço
Chapada Diamantina
Paraguaçu
Rio dos Remédios
Upper
Middle
Lower
Morro do Chapéu
Caboclo
Tombador
Açuruá
Mangabeira
Lagoa de Dentro
Ouricuri do Ouro
Novo Horizonte
Serra da Gameleira
~2500
~2200
~2200
~1600
~1600
~1200
~400
~400
0 m
Fluvio-deltaic and shallow marine
Fluvio-estuarine and shallow marine
Alluvial fans, fluvial, aeolian, estuarine and shallow marine
Fluvial and Deltaic
Aeolian and wadi deposits
Distal alluvial fans
Alluvial fans
Volcanic rocks
Alluvial and aeolian
Mud
Sand
Gravel

Figure 2

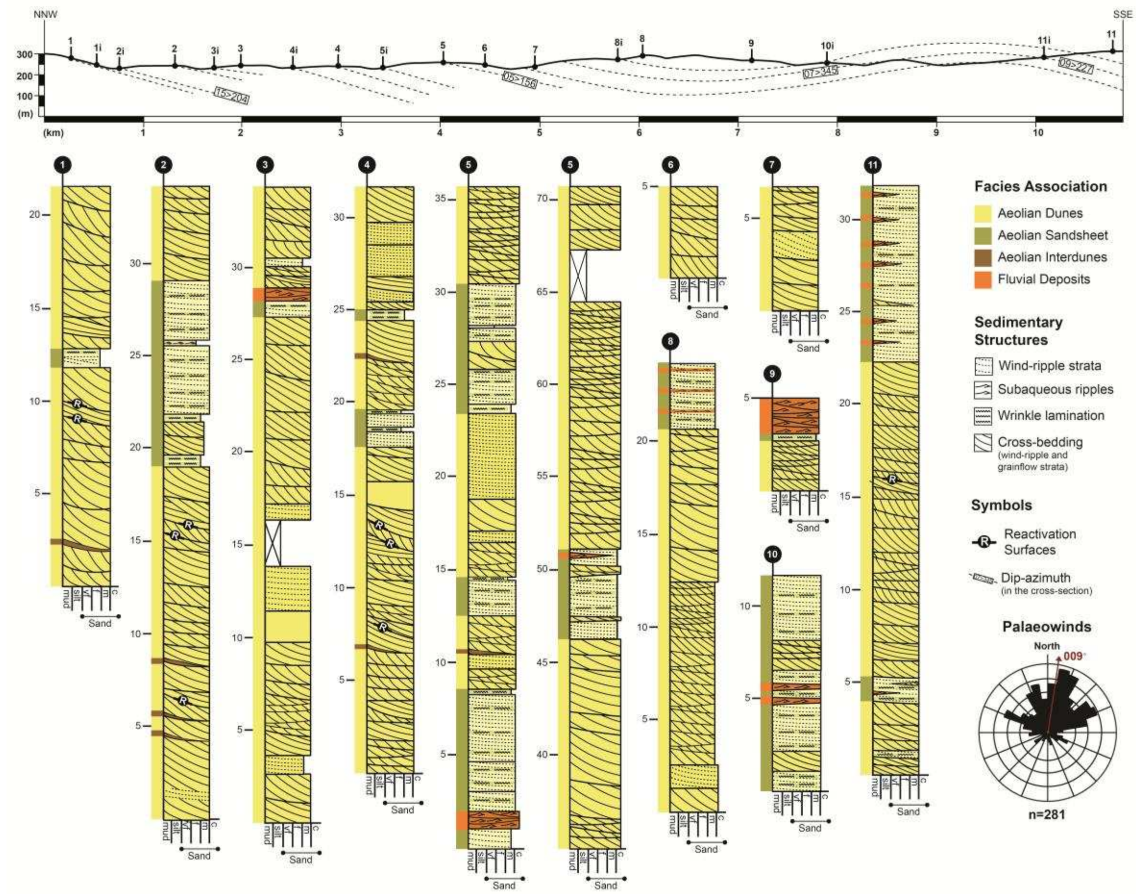

NNW
SSE
Facies Association
Aeolian Dunes
Aeolian Sandsheet
Aeolian Interdunes
Fluvial Deposits
Sedimentary Structures
Wind-ripple strata
Subaqueous ripples
Wrinkle lamination
Cross-bedding (wind-ripple and grainflow strata)
Symbols
Reactivation Surfaces
Dip-azimuth (in the cross-section)
Palaeowinds
North
009°
n=281

Figure 3

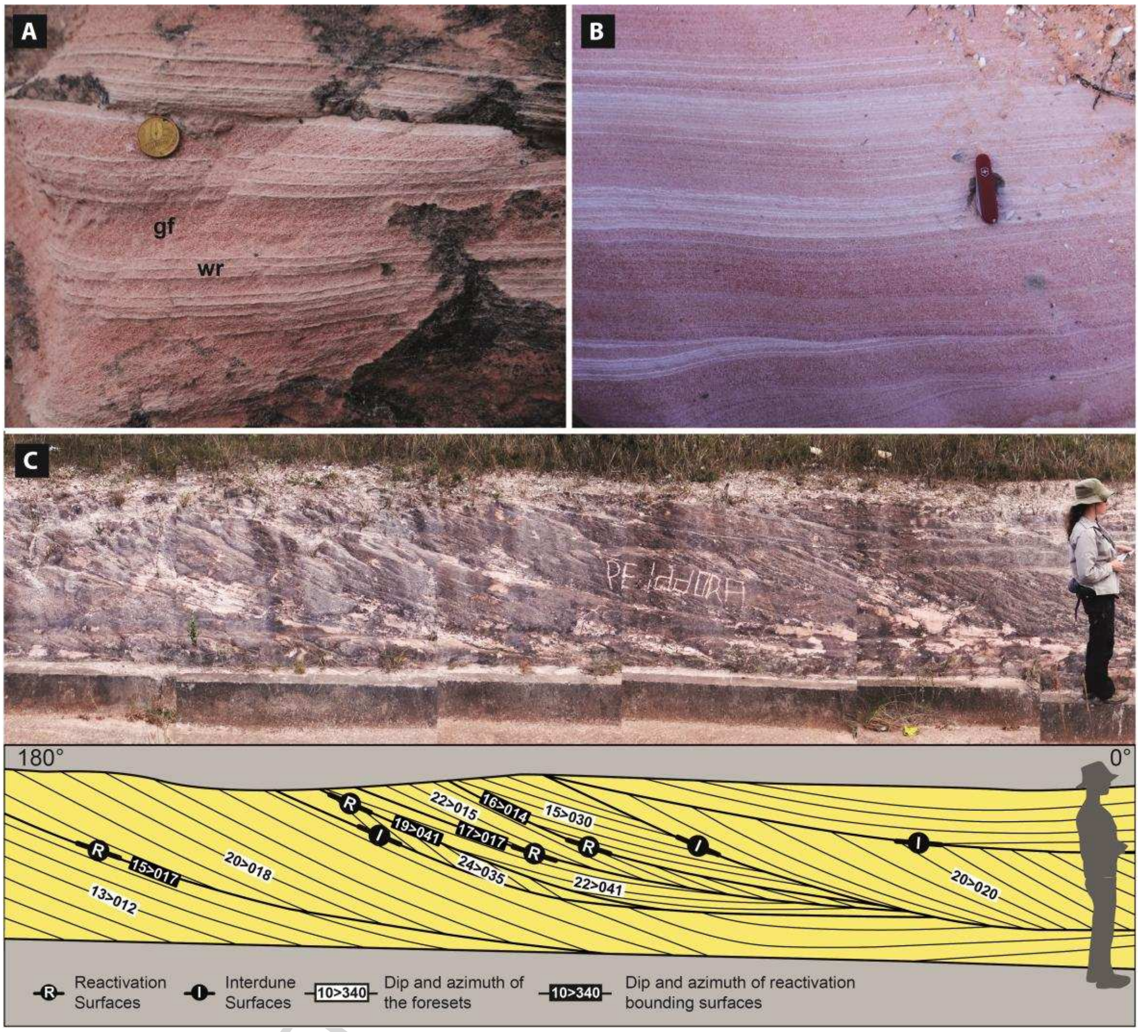
A
gf
wr
B
C
180°
0°
R
I
22>015
16>014
15>030
19>041
17>017
15>017
20>018
24>035
22>041
13>012
20>020
Reactivation Surfaces
Interdune Surfaces
10>340
Dip and azimuth of the foresets
10>340
Dip and azimuth of reactivation bounding surfaces

Figure 4

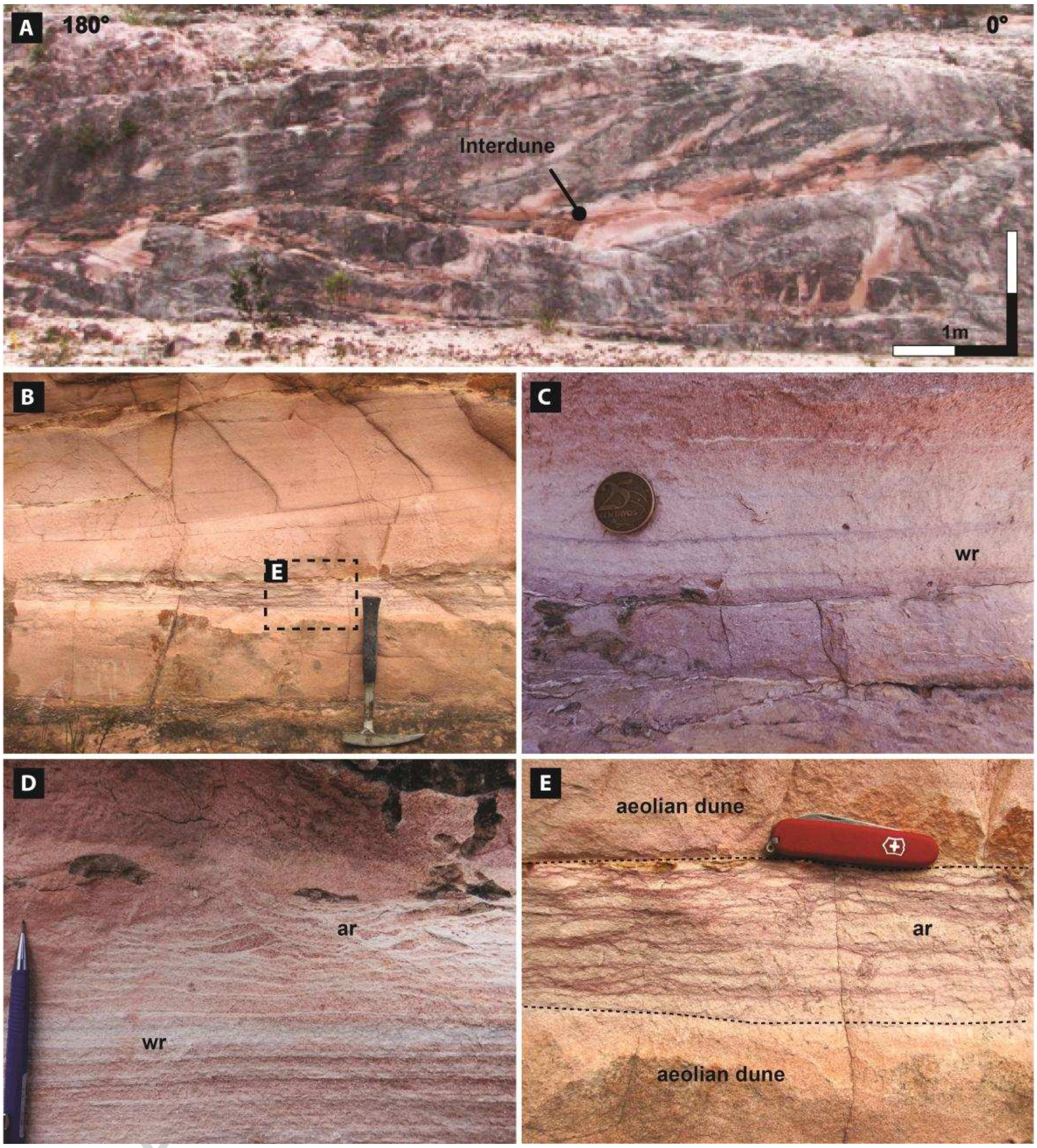
A
180°
0°
Interdune
1m
B
E
C
wr
D
ar
wr
E
aeolian dune
ar
aeolian dune

Figure 5

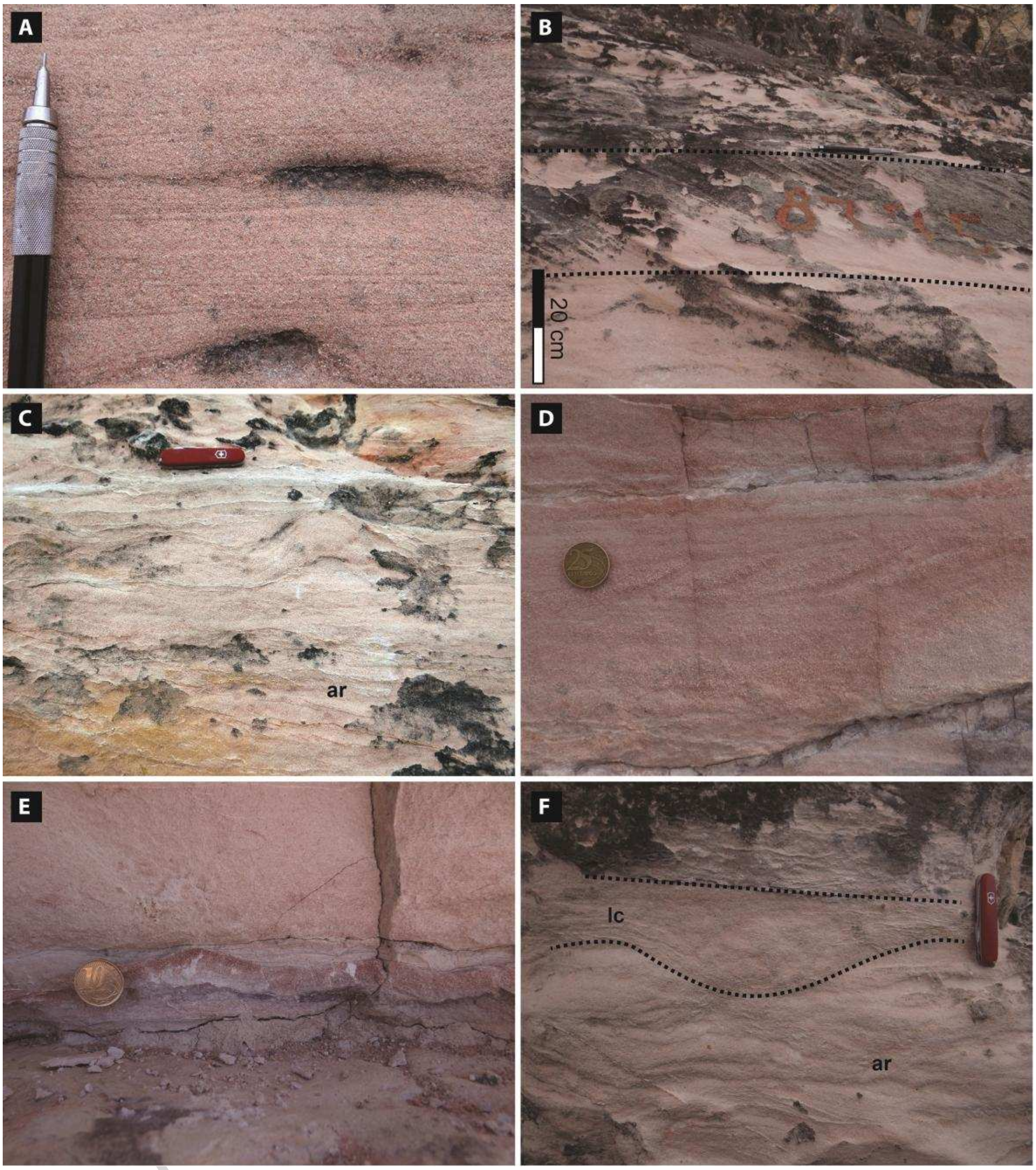

Figure 6

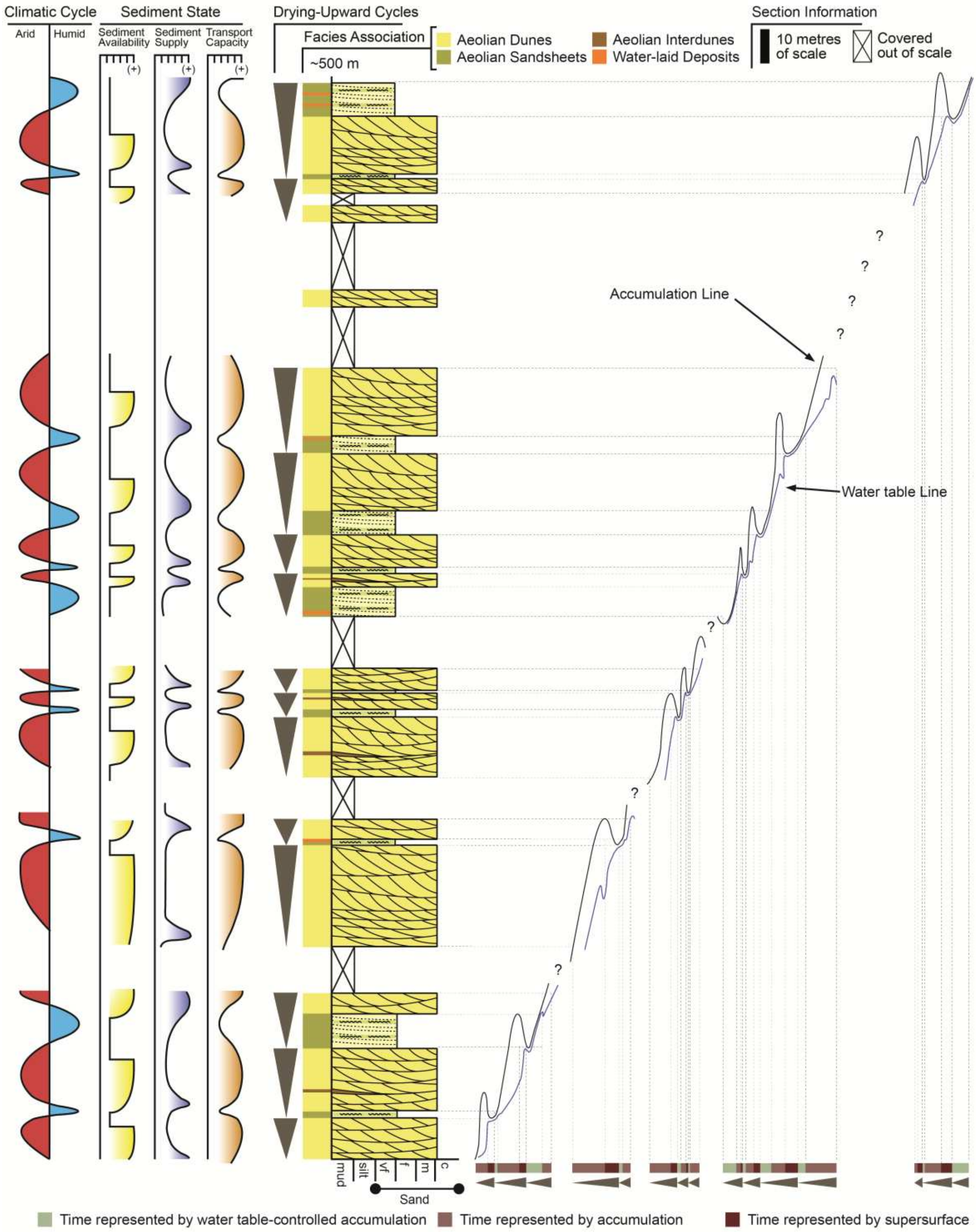

Climatic Cycle
Arid
Humid
Sediment State
Sediment Availability
Sediment Supply
Transport Capacity
(+)
Drying-Upward Cycles
Facies Association
~500 m
Aeolian Dunes
Aeolian Sandsheets
Aeolian Interdunes
Water-laid Deposits
Section Information
10 metres of scale
Covered out of scale
Accumulation Line
Water table Line
mud
silt
vf
f
m
c
Sand
Time represented by water table-controlled accumulation
Time represented by accumulation
Time represented by supersurface

Figure 7

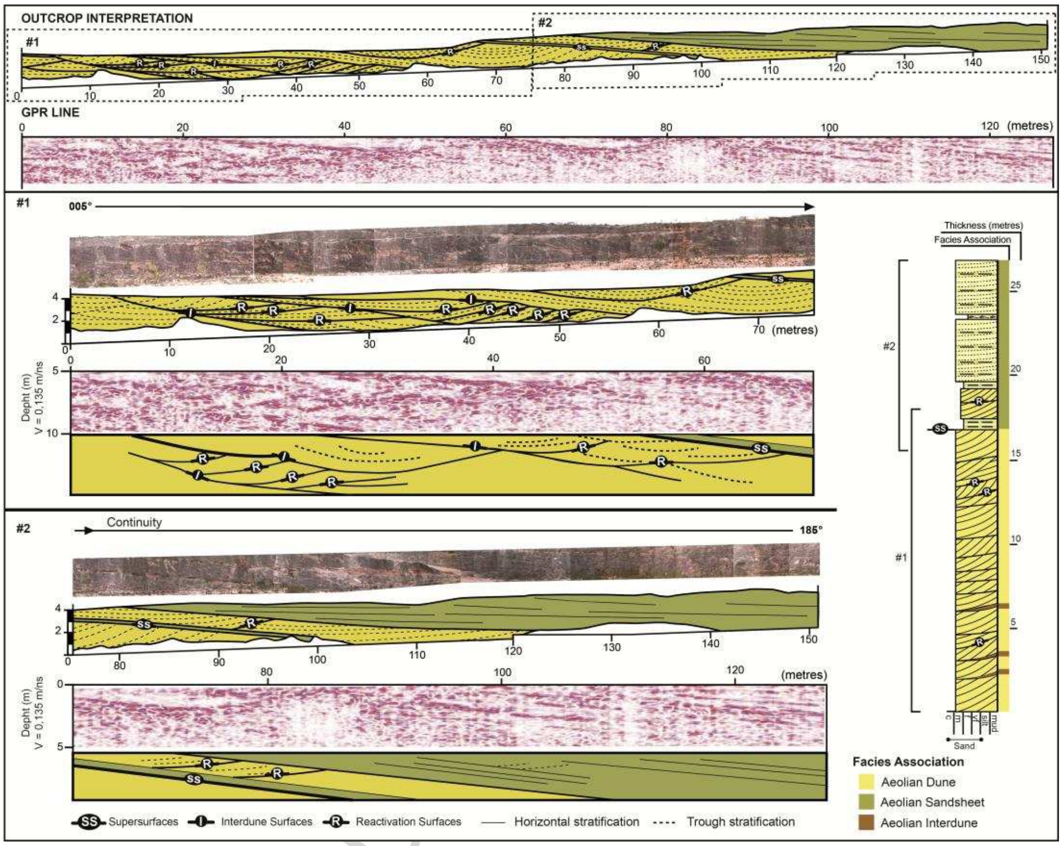

OUTCROP INTERPRETATION
#1
#2
GPR LINE
(metres)
005°
Continuity
185°
Depht (m)
V = 0,135 m/ns
Thickness (metres)
Facies Association
Sand
mud
Supersurfaces
Interdune Surfaces
Reactivation Surfaces
Horizontal stratification
Trough stratification
Facies Association
Aeolian Dune
Aeolian Sandsheet
Aeolian Interdune

Figure 8